A Conceptual 3-D Finite-Element Model of Groundwater Flow and Saltwater Intrusion in the Elk River Aquifer System, California

C.E. Hayler[a] and R.Willis[b]

[a]*Department of Environmental Resources Engineering, Humboldt State University, Arcata, CA, 95521, United States (ceh1@humboldt.edu)*

[b]*Department of Environmental Resources Engineering, Humboldt State University, Arcata, CA, 95521, United States.*

Abstract: The development of groundwater in coastal areas is often associated with concerns about water quality, specifically with the encroachment of saltwater into freshwater aquifers. The objective of this study is to develop a three-dimensional conceptual model of the groundwater flow and saltwater intrusion in the Elk River aquifer system, near Eureka, California, USA. Specifically, the study will identify the major geohydrologic controls affecting the movement of groundwater and saltwater intrusion. The project will involve: (1) a description of the geohydrologic setting, (2) a description of a preliminary three dimensional groundwater flow and transport, numerical model, (3) results of selected model scenarios designed to identify the major geohydrologic controls, and (4) a discussion of possible affects of further development of the aquifer as a source. The results of the study have demonstrated that an increase in the intrinsic permeability causes the saltwater interface to advance approximately 3000 meters seaward from the base-case at equilibrium. A decrease in the intrinsic permeability moved the 50% saltwater isochlor 167 meters inland. Dispersivity and changes in the inland, hydrostatic boundary conditions were found to have a minimal impact on the system. Additional numerical experiments are being conducted to assess the groundwater development potential of the basin.

Keyworks: Groundwater, Saltwater intrusion, Coastal aquifer, Salinity

1 INTRODUCTION

The development of groundwater in coastal regions is often associated with concerns about water quality, specifically saltwater intrusion. As coastal aquifers are developed as a water supply, there exists a potential for saltwater to be drawn towards wells where contamination can occur.

Over the past two decades saltwater intrusion has been studied in many locations including the Jakarta basin [Finney et al., 1992], and Yun Lin basin [Willis et al., 1987]. These investigations typically focus on the impacts of excessive pumping and over reliance of groundwater and the movement of the freshwater-saltwater interface.

Nationally, studies have been undertaken in the Ewa plain, Oahu, Hawaii where water is supplied for irrigation, and domestic use [Oki et al., 1996]. In Florida [Terrazas, 1995], saltwater has intruded into the freshwater aquifers as a result of increased urbanization. In Monterey, California [Essaid, 1990], saltwater intrusion has been found to be a potential problem for shallow wells near the coast. Locally, the Elk River aquifer in Eureka, California, has the potential for saltwater intrusion.

Computational resources have limited the application of most saltwater intrusion studies to two-dimensional models as opposed to quasi three-dimensional or fully three-dimensional models. Two-dimensional models are based on the assumption that flow and transport in the third direction, are averaged values. With the recent advances in computer technology, fully three dimensional, flow and mass transport models have become useful tools in groundwater hydrology.

Accordingly, the objective of this project is to develop a conceptual model of groundwater movement and saltwater intrusion in the Elk River

aquifer using a 3-D, variable density, finite element model.

1.1 Mathematical Model

The mathematical equations used to describe saltwater intrusion in the aquifer system are based on conservation of mass and momentum. The mass balance equation for an aquifer system can be expressed as [Bear, 1972]:

$$\rho S_{op}\frac{\partial p}{\partial t} = -\varepsilon\frac{\partial \rho}{\partial C}\frac{\partial C}{\partial t} - \nabla\cdot(\varepsilon\rho\underline{\upsilon}) + Q_p, \qquad (1)$$

where ρ is density of the fluid (kg/m^3), p is pressure (N/m^2), t is time (sec), ε is porosity (m^3/m^3), $\underline{\upsilon}$ is average velocity (m/sec), C is concentration (kg_{solute}/kg_{fluid}) and Q_p is flow (m^3/sec) into the system. The specific pressure storativity, S_{op}, is defined as $(1-\in)\alpha+\in\beta$ where α [(m sec^2)/kg] is the porous matrix compressibility, and β [(m sec^2)/kg] is the fluid compressibility. The average pore velocity is expressed with Darcy's equation for variable density:

$$\underline{\upsilon} = -\left(\frac{\underline{\underline{k}}k_r}{\varepsilon S_\omega \mu}\right)\cdot(\nabla p - \rho g) \qquad (2)$$

where $\underline{\underline{k}}(x,y,z,t)$ is the solid matrix permeability (m^2), and $k_r(x,y,z,t)$ is the relative permeability to fluid flow (m). Under saturated conditions, k_r=1, and $\underline{\underline{k}}$ is the only permeability constant.

The transport of solute through the aquifer is based on the convection dispersion equation. The exact form of the equation used is: [Bear, 1972]

$$\frac{\partial(\varepsilon\rho C)}{\partial t} = -\nabla\cdot(\varepsilon\rho\upsilon C) + \nabla\cdot[\varepsilon\rho(D_m\mathbf{I}+\mathbf{D})\cdot\nabla C] + Q_p C^* \qquad (3)$$

where C* is the mass fraction solute concentration (kg_{solute}/kg_{fluid}) of a fluid source and **I** is an identity matrix.The hydrodynamic dispersion is the sum of the mechanical dispersion **D** and molecular diffusion, D_m.

The approximate density model is a first order Taylor series expansion about a base density. For solute transport, this can be expressed as,

$$\rho = \rho(C) \approx \rho_0 + \frac{\partial\rho}{\partial C}(C - C_0) \qquad (4)$$

where ρ_0 is the base fluid density at a base concentration, C_0. The change in density with respect to the change in concentration which is approximately 700 kg/m^3 for saltwater intrusion [Oki et al., 1996].

1.2 Numerical Model

The solutions of the flow and mass transport equations are approximated with the Galerkin, finite element method.

The pressure and concentration are approximated as the finite series,

$$p \approx \tilde{p} = \sum_{i=1}^{NN} N_{i_{x,y,z}}\tilde{p}(t) \qquad (5)$$

$$C \approx \tilde{C} = \sum_{i=1}^{NN} N_{i_{x,y,z}}\tilde{C}(t) \qquad (6)$$

where N_i are the basis functions and $\tilde{p}$ and $\tilde{C}$ are the nodal values of the pressure and concentration.

The Galerkin approach requires that the residual error associated with the finite series approximations (Equations 5 and 6) are orthogonal to each of the basis, or weighting functions, N_i, or [Lapidus and Pinder, 1982]:

$$\int_V R(x,y,z,t)N_i(x,y,z)dV = 0, \forall i \qquad (7)$$

where $N_i(x,y,z)$ are the basis functions, $R(x,y,z,t)$ is the residual error, and V is the volume of the region. Substituting Equations 5 and 6 into 7, yields:

$$\int_V N_i L_p\{\tilde{p}\}dV = 0, \forall_i \qquad (8)$$

$$\int N_i L_C\{\tilde{C}\}dV = 0, \forall_i \qquad (9)$$

2 STUDY AREA

The Humboldt Community Services District (HCSD) is currently interested in the further development of the Elk River aquifer to augment their water supply and reduce their dependence on other sources. The HCSD currently extracts up to 1000 gallons per minute from two wells in the Elk River aquifer. Future plans are to (1) increase

pumping rates to 1000 gallons per minute for both wells and (2) develop a new well with the capability of pumping 1000 gallons per minute. The HCSD has a total projected demand of 3000 gallons per minute.

Elk River valley lies south of Eureka, CA, extending southeast from Humboldt Bay. It is bordered on the south by Humboldt Hill with an elevation of 180 meters (600 feet), and on the north by coastal hills extending 120 meters (400 feet) above sea level (Figure 1). The Elk River basin comprises an area of 114.5 km^2 extending inland approximately 10 km. The southern boarder of the valley along Humboldt Bay is King Salmon.

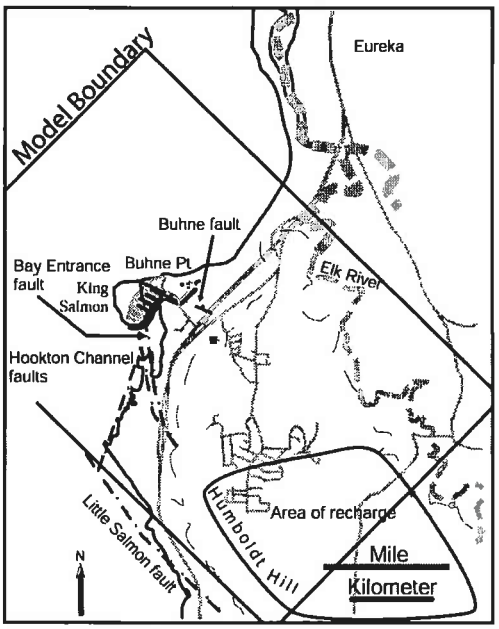

Figure 1 Map of Humboldt Hill and Elk River Valley near Humboldt Bay, California.

The historical head was observed in the aquifer during the construction of South Bay and Spruce Pt. wells. The pressure was measured on August 8, 1988, at 4.0 to 4.5 psi corresponding to head height of 2.8 to 3.2 meters. At the onset of a pump drawdown test the head was estimated at 3.5 meters on August 17, 1988.

The head at Spruce Pt. well was measured on July 25, 1988 at the beginning of a pump test at the conclusion of construction. The location of Spruce Pt. well is estimated between 4.6 meters and 6.1 meters above sea level (USGS 7.5 minute map). The static level of the well was measured at 5.5 meters below the surface, corresponding to approximately 0 meters, or sea level.

2.1 Geology

Elk River Aquifer is comprised of layers of sand and gravel with minor amounts of silt and clay. Wells in the area are approximately 122 meters (400 feet) deep in a sand and gravel layer located between silt and clay layers. The confining top layer is comprised of blue clay, 30.5 meters (100 feet) thick. The sand and gravel area is exposed to the surface at the top of Humboldt Hill where the majority of recharge into the system occurs [Woodward-Clyde Consultants, 1980].

Humboldt Hill is a faulted anticline, a result of the Little Salmon fault, where the southern portion of Humboldt Bay has been thrust under the Humboldt Hill area. This southern fault results in an apparent impermeable boundary, that extends westward along the Bay Entrance fault [Woodward-Clyde Consultants, 1980].

A small thrust fault, Buhne Point fault, intersects the Bay Entrance fault near Buhne Point (Figure 1). The inland extent of this fault is unknown, although it is not likely to extend past Highway 101.

Leakage of saltwater into the aquifer is assumed to occur as the aquifer extends west past the coast line, creating a saltwater boundary on the ocean side. The inland boundary is subjected to freshwater infiltration and percolation. The flow of water and the transport of solute through the aquifer is expected to be highly influenced by faulting in the area

3 MODEL APPLICATION

The inland boundary condition across the width of the system (located 3250 meters from the coastline) is a hydrostatic pressure distribution plus an additional 10 meters to induce a gradient across the system. Freshwater may enter the system along the entire face, however the lower layer of mud and silt will not permit a significant amount of inflow compared to the sand and gravel layer. The sand and gravel layer is in contact with the inland boundary condition at the top 900 meters.

The saltwater boundary (located 3750 m from the coastline), is specified as hydrostatic at sea level. The concentration of fluid at this boundary is specified with the mass fraction of seawater equal to 0.0375. Saltwater is allowed to flow in through the entire face of the system.

Table 1 Permeabilities and dispersivities for scenarios.

Scenario	Sand and gravel				Upper and lower silt and clay			
	Intrinsic permeability (m^2)		Dispersivity (m)		Intrinsic permeability (m)		Dispersivity (m^2)	
	Max	Min	Max	Min	Max	Min	Max	Min
1	5.00 E-09	5.00E-10	75.0	7.5	5.00E-13	5.00E-14	0.75	0.075
2	5.00E-08	5.00E-09	75.0	7.5	5.00E-13	5.00E-14	0.75	0.075
3	5.00E-10	5.00E-11	75.0	7.5	5.00E-13	5.00E-14	0.75	0.075
4	5.00E-11	5.00E-12	75.0	7.5	5.00E-14	5.00E-15	0.75	0.075
5	5.00E-09	5.00E-10	100.0	10.0	5.00E-13	5.00E-14	1.00	0.100
6	5.00E-09	5.00E-10	37.5	3.8	5.00E-13	5.00E-14	0.375	0.0375
7	5.00E-09	5.00E-10	75.0	7.5	5.00E-13	5.00E-14	0.75	0.075
8	5.00E-08	5.00E-09	75.0	7.5	5.00E-13	5.00E-14	0.75	0.075
9	5.00E-10	5.00E-11	75.0	7.5	5.00E-13	5.00E-14	0.75	0.075
10	5.00E-09	5.00E-10	100.0	10.0	5.00E-13	5.00E-14	0.100	0.100
11	5.00E-09	5.00E-10	37.5	3.8	5.00E-13	5.00E-14	0.375	0.0375

3.1 Description of Scenarios

The system is a sloped aquifer with three layers. The three layers differ with respect to the intrinsic permeability and dispersivity. The top layer represents a layer of silt, clay and bay mud with permeabilities and dispersivities lower than the middle layer. The middle layer represents sands and gravels where water extraction occurs. The intrinsic permeabilities and dispersivities are higher in this layer. The lower layer represents silts and clays, and is similar to the upper layer. Values for intrinsic permeability and dispersivity for each scenario are in Table 1.

The system is sloped for the first 3000 meters moving inland towards the coastline. In this region the direction of maximum permeability is sloped downward at approximately 3.5°. The last 4000 meters of the system is not sloped, and the direction of maximum permeability is horizontal. Eleven scenarios are used to evaluate changes in the system when the dispersivity and intrinsic permeability are varied. The first 6 scenarios do not include faults and are contrasted with the remaining 5 scenarios where faults are included.

4 MODEL RESULTS

Scenarios one and seven are base case scenarios, without and with faults, respectively. Scenarios 2 through 5 were started from scenario 1; scenario 6 through 12 were started from scenario 7. Steady state was reached for the pressure solution in all scenarios. Due to the high computational demand, the concentration solution was not run to steady state, however simulation times were long enough to evaluate the response of the system for each scenario.

4.1 Base Case Scenarios

Two different scenarios were used to evaluate changes in the system with and without faults. Scenario 1 was used as a base case for comparison with scenarios without faults. Scenario 7 was used as a base case scenario with faults, and also compared to scenario 1 to assess the affect of faulting in the system.

The total simulation time of scenario 1 was 300 years. The initial condition was hydrostatic pressure distribution with head equal to sea level. The pressure and concentration converged to a steady-state solution at 50 and 250 years respectively. The change in stored fluid due to a change in pressure is $3.62 \times 10^{-11} m^3/sec$ and $-1.8063 \times 10^{-1} m^3/sec$ due to changes in concentration. Scenarios 2 through 6 were started from scenario 1.

Saltwater has intruded in the sand and gravel layer with a mixing zone between 750 and 1750 meters (Figure 2). The velocity field shows flow into the system from both boundaries, and the location of the interface is consistent with mixing zone from the concentration solution. The heads in the system decrease from 10 meters to 0 meters at the saltwater boundary.

Scenario 7 was started from scenario 1 at 10 days of simulation time allowing the pattern of flow to develop with the faults in the system. The total simulation time is 150 years. This scenario is used

as a base case for scenarios 8 through 11. The change in stored fluid due to a change in pressure is $3.823 \times 10^{15} m^3/sec$ and -3.535 m^3/sec due to change in concentration. Three cross sections at x = 600, 1500, and 3600 meters are used to evaluate the extent of saltwater intrusion into the system.

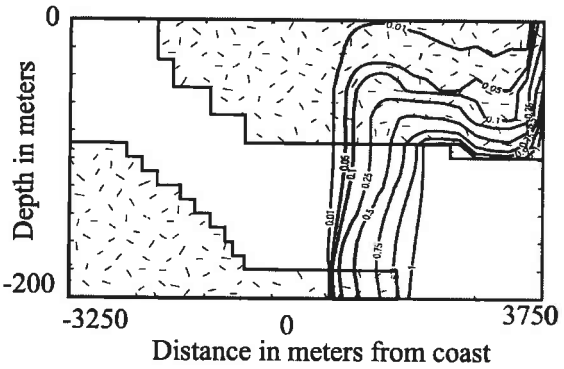

Figure 2 : Concentration isoclores for base case scenario.

4.2 Increased Intrinsic Permeability

An increase in permeability resulted in a change in the pattern of flow. In scenario 2 (Figure 3), fresh water exits the system in the sand and gravel layer. This change resulted in pushing the saltwater interface towards the saltwater boundary. The distance from the datum to the 1% concentration line increased from 583 meters in scenario 1 to 3400 meters in scenario 2. The 50% and 100% concentration lines moved towards the saltwater boundary

The increased permeability increases variation in head across the width of the system with faults . Flow is also increased out of the system pushing the saltwater front towards to the saltwater boundary. This suggests one order of magnitude increase is too large to represent historically observed data.

4.3 Decreased Intrinsic Permeability

Three scenarios evaluated the affect of decreased permeability: 3, 4 and 8. Scenarios 3 and 8 decreased the permeability in the sand and gravel layer by one order of magnitude; scenario 4 decreased the permeability of the middle sand and gravel and both silt and clay layers by two and one order of magnitude respectively.

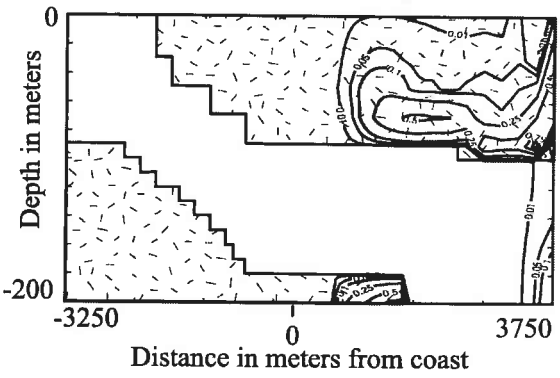

Figure 3 Concentration isoclores with increased intrinsic permeability.

The concentration also showed a difference for all three scenarios. In scenario 3 the distance from datum to the 1% concentration line is similar to scenario 1. The 50% concentration line is also the same as scenario 1 at 110 meters deep, however at 180 meters deep it advances 167 meters inland compared to scenario 1. The 100% concentration line moves 50 meters towards the saltwater boundary, while at 180 meters deep, it moves inland 50 meters. This suggests a decrease in intrinsic permeability decreases the degree of saltwater intrusion by limiting flow in the system.

4.4 Dispersivity

The dispersivity was varied in four different scenarios: without faults in scenarios 5 and 6 and with faults in 10 and 11. The pressure solution was not affected by changes in dispersivity, however there were changes in head due to changes in concentration. In scenarios 5 and 6, the 1% concentration line did not move compared to scenario 1 at 180 meters deep. At 110 meters deep, the 1% concentration line moved inland approximately 100 meters for both scenarios.

4.5 Pressure Solution

The pressure solution is most impacted by a high intrinsic permeability. The largest difference from scenario 7 for the pressure solution occurs in scenario 8. The pressure increases near the South Bay well and decreases at the Spruce Pt. well. This pattern of flow is most similar to the observed record at each well. Scenarios with lower intrinsic permeabilities have a smaller difference of pressure along the width of the system

4.6 Velocity

The pattern of flow through the aquifer is reduced where the faults cross the system (Figure 4). Near the intersection of the South Bay and Buhne faults there are large velocities throughout the non-restricted area. Flow through this point increased the circulation and reduce the concentration of saltwater.

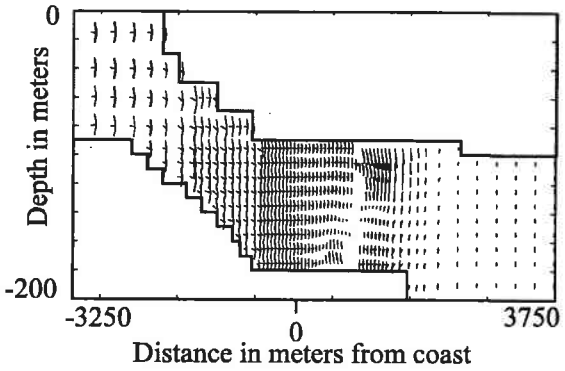

Figure 4: Velocity vectors with faults in the system.

5 CONCLUSIONS

Intrinsic permeability has a major influence over groundwater flow and saltwater intrusion in the Elk River aquifer. The extent of saltwater intrusion varies greatly with permeability changes of one order of magnitude. An increase in the intrinsic permeability results in the saltwater front moving towards the saltwater boundary.

The presence of faulting across the width of the aquifer changes the character of the system. With faults included, the system becomes a fully three-dimensional system.

Diffusivity and molecular diffusion had minimal impact on the extent of saltwater intrusion as compared to the influence of the intrinsic permeability.

Changes in the inland hydrostatic boundary condition after the model was run to steady state resulted in no change in the system. Results from starting the numerical model from an initial condition of hydrostatic pressure across the aquifer resulted in infeasible solutions for inland boundary conditions smaller than 10 meters. Simulations started from hydrostatic conditions in the aquifer with an inland boundary condition greater than 10 meters resulted in heads near the well that far exceed the observed pressures.

6 RECOMMENDATIONS

A pump draw-down test should be done to estimate the permeability of the aquifer. Understanding the characteristics of the aquifer can lead to development of a refined model, better representing the Elk River aquifer.

7 REFERENCE

Bear, J. *Dynamics of Fluids in Porous Media.* General Publishing Company, Ltd., 30 Lesmill Road, Don Mills, Toronto, Ontario, 1972.

Essaid, H.I. A multilayered sharp interface model of coupled freshwater and saltwater flow in coastal systems: Model development and application. *Water Resources Research,* 26(7):1431-1454, 1990.

Finney, B.A., Sasuhadi, and R. Willis, . Quasi-three-dimensional optimization model of Jakarta basin. *Journal of Water Resources Planning and Management.,* ASCE, 118(1):18-31, 1992.

Lapidus, L., and G.F. Pinder *Numerical Solution of Partial Differential Equations in Science and Engineering.* John Wiley & Sons, Inc, 1982.

Oki, D.S.,W.R. Souza, E.L. Bolke, and G.R. Bauer, Numerical analysis of ground-water flow and salinity in the Ewa area, Oahu, Hawaii. Open-File Report, 96-442, U.S. Geological Survey, 1996.

Terrazas, M. Saltwater intrusion: Florida's underground movement. *Journal AM CITY,* 110(2):6pp, 1995.

Willis, R., B.A. Finney, and P.L.-F. Liu, Optimal control of saltwater intrusion: the Yun Lin Basin, Taiwan. *Systems analysis in water quality management: Proceedings of symposium held in London, U.K.* Pergamon Press, New York, 1987.

Woodward-Clyde Consultants, Evaluation of he potential for resolving the geologic and seismic issues at the Humboldt Bay Power Plant Unit. Technical Report 13976G-6520, 5216.1, 1980.